Mach reflection in steady flow. I. Mikhail Ivanov's contributions, II. Caltech stability experiments

Hans G. Hornung

Citation: AIP Conference Proceedings **1628**, 1384 (2014); doi: 10.1063/1.4902753
View online: http://dx.doi.org/10.1063/1.4902753
View Table of Contents: http://scitation.aip.org/content/aip/proceeding/aipcp/1628?ver=pdfcov
Published by the AIP Publishing

Mach Reflection in Steady Flow. I. Mikhail Ivanov's Contributions, II. Caltech Stability Experiments

Hans G. Hornung

Graduate Aerospace Laboratories, California Institute of Technology, USA

Abstract. To honor the memory of our friend and colleague Mikhail Ivanov a review of his great contributions to the understanding of the various phenomena associated with steady–flow shock wave reflection is presented. Of course, he has contributed much more widely than that, but I will restrict myself to this part of his work, because it is what I understand best. In particular, his computational and experimental demonstration of hysteresis in the transition between regular and Mach reflection, and his resolution of the difficulties associated with the triple point in weak Mach reflection in terms of the effects of viscosity and heat conduction are reviewed. Finally, some experimental results are presented that demonstrate that, in the dual–solution domain, Mach reflection is more stable than regular reflection.

Keywords: Mach reflection, hysteresis, viscosity
PACS: 51

MIKHAIL IVANOV'S CONTRIBUTIONS

Hysteresis in Transition Between Regular and Mach Reflection

Background

When a plane oblique shock impinges on a wall or symmetry plane in inviscid steady supersonic flow parallel to the wall, the flow is deflected toward the wall. The boundary condition at the wall, that the flow must be parallel to the wall, brings about a reflected shock that deflects the flow back to the undisturbed flow direction. This is illustrated in Fig. 1, left, showing as an inset a schematic of the incident and reflected shock waves separating states (1), (2), and (3). The oncoming flow (1) is processed by the incident shock to take it to state (2) which must lie on the curve (often referred to as shock polar) joining (1) and (2) in the deflection–pressure (θ–p) plane, as determined by the shock jump conditions. Similarly, from (2), the reflected shock produces state (3) which must lie on the curve joining (2) and (3). Since the deflection in state (3) must be zero, the intersection of the second curve with the p–axis determines (3). This is called regular reflection.

As the shock angle is increased, there comes a point when the reflected–shock polar does not reach the p–axis any more. This makes it necessary that the reflection point moves away from the wall, permitting the flow direction in region (3) to have a wall–normal component. A third, nearly normal shock (Mach stem) appears between the triple point and the wall. On both sides of the streamline issuing from the triple point, p and θ must have the same values, and the Mach stem must be mapped into part of the incident shock polar, so that the five points shown in the physical plane inset into Fig. 1, right, are mapped into the correspondingly numbered points in the (θ–p) plane. The configuration in Fig. 1, right is called Mach reflection.

For shock angles larger than that at which the reflected polar is tangent to the p–axis, regular reflection is not possible. The tangency point is shown in Fig. 2, left. It is called the detachment condition, shock angle α_D. The condition at which the two shock polars intersect on the p–axis, called the von Neumann condition, is shown in Fig. 2, right. For shock angles smaller than that at the von Neumann condition, α_N, Mach reflection is not possible. However, for $\alpha_N > \alpha > \alpha_D$, both regular and Mach reflection are possible, see Fig. 3, left. The shock angles for the two special conditions depend on free stream Mach number M_∞ and specific heat ratio γ. In Fig. 3, right, their dependence on M_∞ is shown for $\gamma = 1.4$.

As may be seen in Fig. 4 left, the flow in the immediate vicinity of a regular reflection point does not exhibit a length scale. This is as it should be, since no information about the scale of the boundary conditions such as the length of the wedge can reach the reflection point in this entirely supersonic flow. However, in Mach reflection, see Fig 4, right, a subsonic pocket exists downstream of the Mach stem. The leading characteristic from the trailing edge of the wedge

Proceedings of the 29th International Symposium on Rarefied Gas Dynamics
AIP Conf. Proc. 1628, 1384-1393 (2014); doi: 10.1063/1.4902753

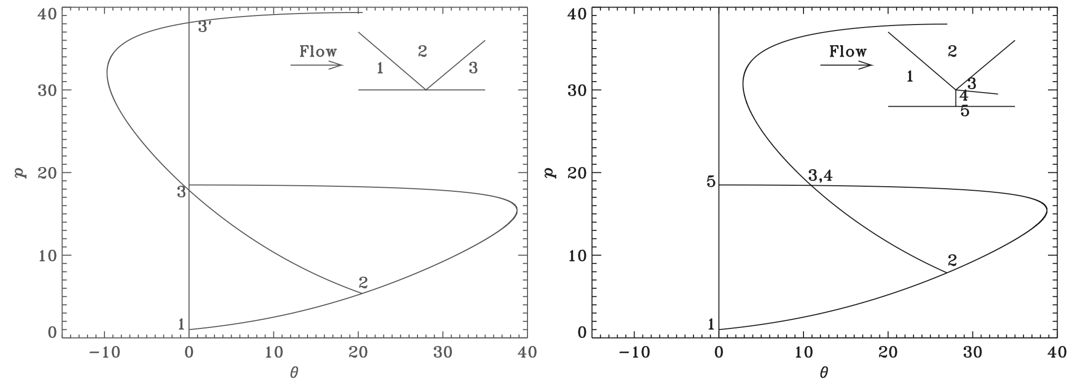

FIGURE 1. Left: Regular reflection. The numbers on the axes are degrees for θ and p is the pressure normalized by the pressure in region(1). All examples here are for $M_\infty = 4$ and $\gamma = 1.4$. Right: Mach reflection. Reproduced by permission from H. G. Hornung: On the stability of steady–flow regular and Mach reflection, Shock Waves 7:123–125, license no. 3424380426949.

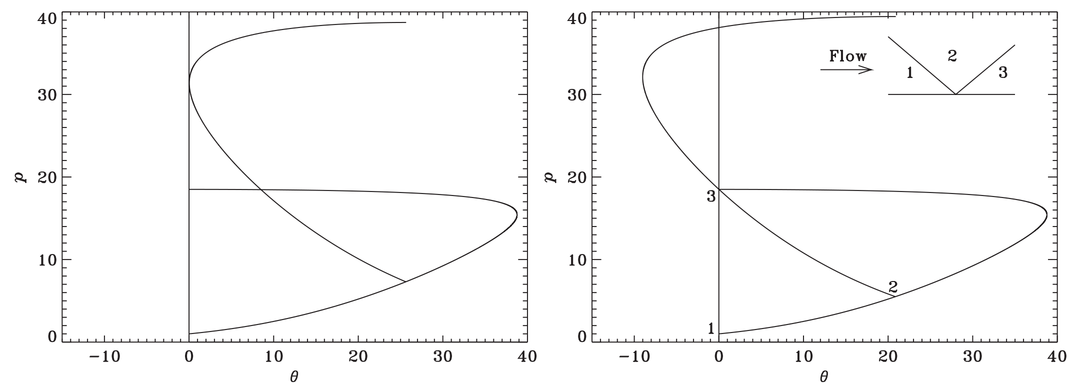

FIGURE 2. Left: Detachment condition. Right: von Neumann condition. Reproduced by permission from H. G. Hornung: On the stability of steady–flow regular and Mach reflection, Shock Waves 7:123–125, license no. 3424380426949.

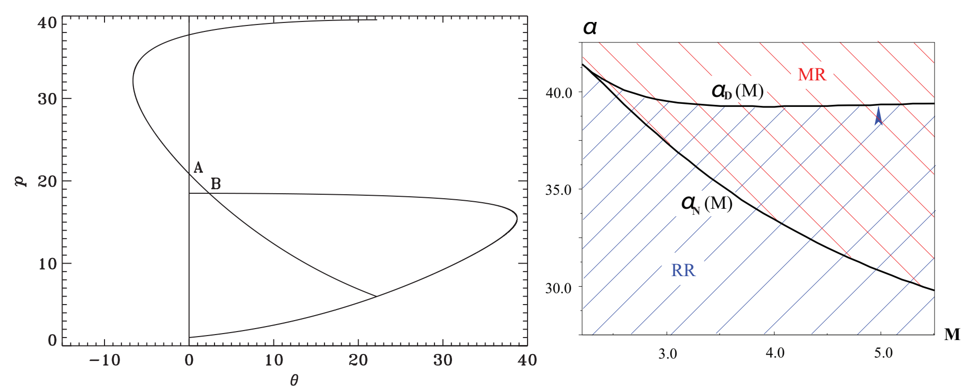

FIGURE 3. Left: Between the von Neumann and detachment conditions both regular (RR) and Mach reflection (MR) are possible, shown by points A and B. Reproduced by permission from H. G. Hornung: On the stability of steady–flow regular and Mach reflection, Shock Waves 7:123–125, license no. 3424380426949. Right: Dependence of detachment condition (upper curve, α_D) and von Neumann condition (lower curve, α_N) on Mach number for $\gamma = 1.4$. The region between the two curves is referred to as the dual–solution domain.

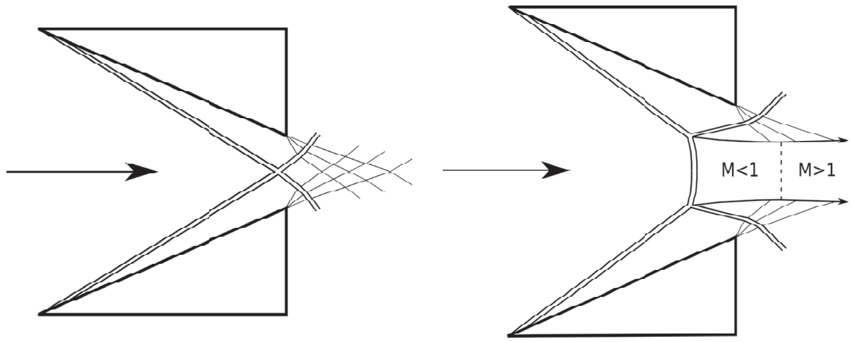

FIGURE 4. In experiments, a symmetrical arrangement is used, in order to avoid the viscous boundary layer effects associated with a physical wall. Left: In regular reflection, the flow is supersonic throughout, so that no knowledge of the scale of the experiment (*e. g.*, length of shock-generating wedge) reaches the reflection point. Right: In Mach reflection, a subsonic pocket exists downstream of the Mach stem, allowing information about the length of the wedge to reach the reflection point, thus giving the Mach stem a scale.

reaches this subsonic pocket, so that information about the length of the wedge does reach the reflection point. This means that, once Mach reflection exists, the condition that information reaches the reflection point, necessary for its existence, is given. Arguing along such lines Hornung *et al.*, 1979[1] suggested that MR is more stable than RR in the dual–solution domain, and that, in the absence of large disturbances, an increase of α from below α_N should be accompanied by a persistence of RR up to $\alpha = \alpha_D$, at which point a sudden jump to MR should occur. Conversely, a decrease of α from above α_D should be accompanied by a smooth decrease of the Mach stem height until, at $\alpha = \alpha_N$, it disappears.

Hornung and Robinson, 1982[2] then tried to test this hysteresis hypothesis experimentally at four different Mach numbers and failed completely. In all cases, a smooth transition between RR and MR occurred very near $\alpha = \alpha_N$ independently of the direction of α change. For their results, see Fig. 12.

Contributions of Mikhail Ivanov and His Team

This is where Mikhail Ivanov came into the picture. During an extended visit to Aachen he became intrigued by the situation and decided to attempt to test the hysteresis hypothesis computationally. By changing the wedge angles in a symmetrical arrangement he found that hysteresis did indeed occur. Examples of his computational results are shown in Fig. 5. The results were published in Ivanov *et al.*,1995[3]. The success of the computations then motivated Ivanov and his team of co–workers to use the extensive experimental facilities of ITAM at Novosibirsk to tackle the various aspects of transition in a massive effort (see [5], [4], [6]). Figure 6 shows an example of the many quality schlieren images from this work. The experimental investigations included studies of the degree to which the jump in Mach stem could approach the detachment point, see Fig. 7 left, and the sudden jumps in pitot pressure at transition, see Fig. 7 right. It also included the study of the three–dimensional nature of the Mach reflection structure using a laser light sheet method to resolve the flow in the spanwise direction, see Fig. 8 left. They also showed that the aspect ratio of the wedges has a strong effect on the slope of s with α, see Fig. 8 right, but the transition points are independent of the aspect ratio, provided that it is sufficiently large.

At the same time, numerous further computational investigations were undertaken by the team. One of these tackled the problem using a statistical simulation [7]. The experimental work on three-dimensionality was also accompanied by computations [8]. The effect of free–stream disturbances was investigated computationally by Kudryavtsev *et al.*[9] and experimentally by Ivanov *et al.*[6].

The reflection transitions of detonation waves and effects of chemical reactions were computed by Trotsyuk *et al.*[10]. By examining the shape of the dual–solution domain in Fig 3, right, it may be seen that one can cross this domain at constant α by varying the Mach number. This is also accompanied by hysteresis as was shown computationally by Ivanov *et al.*[11]. Of course, the shock reflection in the case of a plane overexpanded jet produces similar phenomena, and this was demonstrated computationally by Hadjaj *et al.*[12]. Additional computational work by the group may be found in [13], [14], [15].

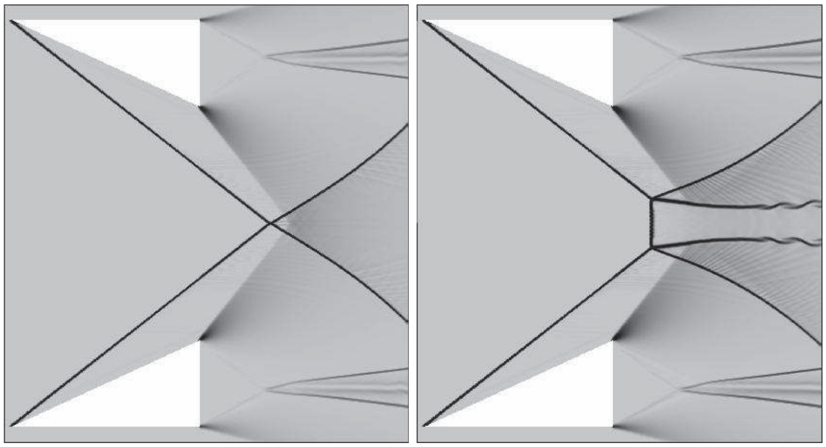

FIGURE 5. Examples of Ivanov's computational results. Depending on the direction of wedge angle variation, these two configurations occur at identical shock angle $\alpha = 38^\circ$ in the dual–solution domain. $M_\infty = 4$, $\gamma = 1.4$. Reproduced from Ivanov *et al.* [4] with permission from Springer Verlag, license no. 3421551251720.

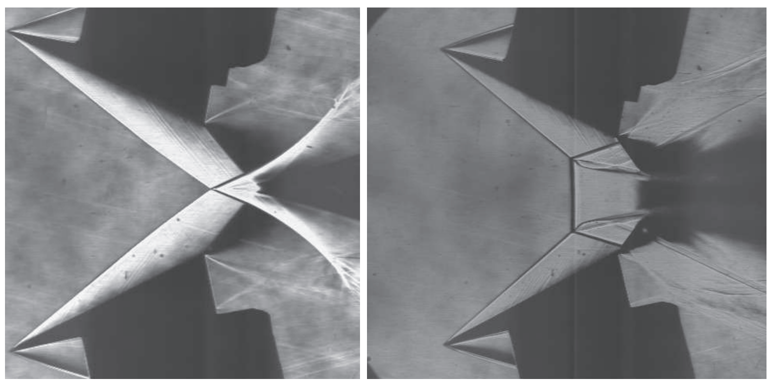

FIGURE 6. Schlieren images of two experiments. Left: $M_\infty = 4$ $\alpha = 39.7^\circ$. Right: $M_\infty = 4$, $\alpha = 40^\circ$, both very close to the detachment point. Reproduced from Ivanov *et al.* [4] with permission from Springer Verlag, license no. 3421551251720.

The body of work, from which only a few examples are given here, represents the most complete and extensive investigation into the various aspects of steady–flow Mach reflection. The ITAM team under the leadership of Mikhail Ivanov deserves enormous credit for it. Among the other research groups that have produced experimental results on some of the aspects that were studied by the ITAM researchers the most notable is the work of Sudani *et al.*[16], and, more recently, of Mouton *et al.*[17].

The Effect of Viscosity and Heat Conduction on Mach Reflection

According to inviscid three–shock theory the incident and reflected shock polars do not intersect with each other when the incident shock is sufficiently weak ($M_\infty < 2.2$ for $\gamma = 1.4$), suggesting that no triple–point solution then exists. Nevertheless, experiments such as those of Smith 1946[20] seem to show a quite clear triple point, see Fig. 9, left. Guderley first obtained an inviscid solutions to this problem that required the existence of a fourth wave, an expansion, to be centered at the triple point. In the polar diagram this expansion connects the incident shock polar to the sonic point on the reflected shock polar, see Fig. 10.

While this inviscid solution removes the difficulty, the real situation involves viscous and heat conduction effects, and it was suggested by Sternberg[18] that, by including them, a resolution would be possible with three shocks.

Mikhail Ivanov decided to use the considerable expertise of his team in Direct Simulation Monte Carlo (DSMC)

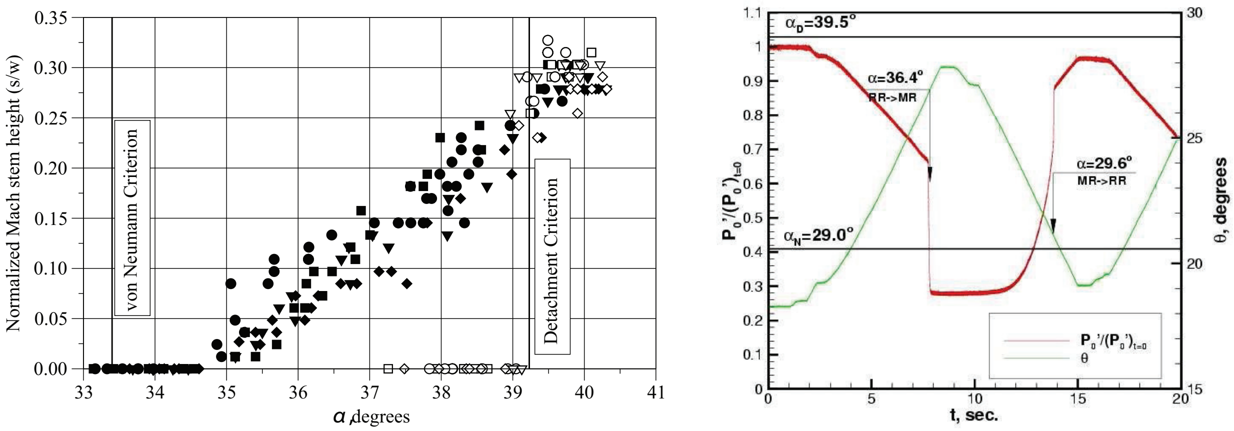

FIGURE 7. Left: Variation of the Mach stem height s normalized by wedge length w with Shock angle α at $M_\infty = 4$. Open symbols show behavior during increasing α, filled symbols during decreasing α. This is a very nice demonstration of the hysteresis and, because the jump in s/w occurs very near the detachment point, indicates the low disturbance level of the wind tunnel. Right: Variation of pitot pressure with time as wedge angle is changed, indicating the values of α at which the jump in pitot pressure occurs at transition.

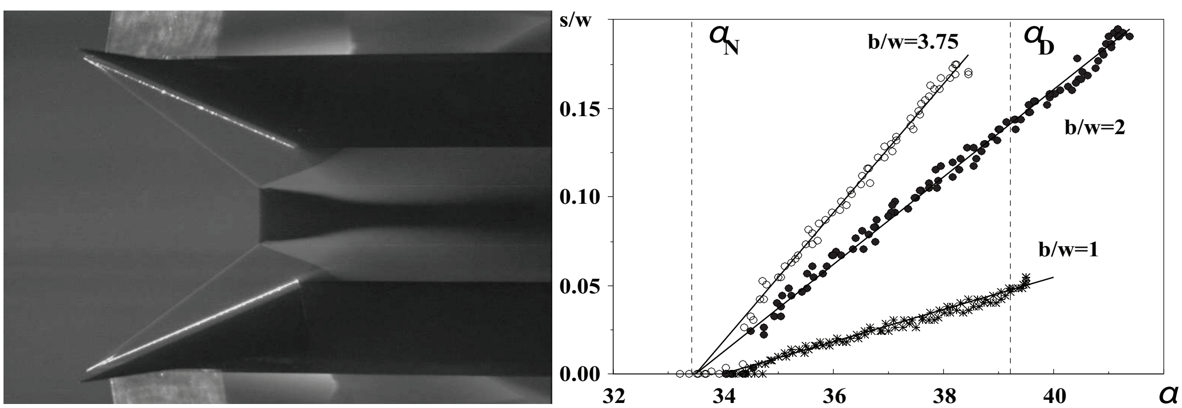

FIGURE 8. Left: An example of the use of the laser sheet method for studying the three–dimensional structure of the Mach reflection. Right: Effect of aspect ratio w/b on the rate of decrease of s/w as α is reduced.

methods and in computational Navier–Stokes techniques to tackle this problem. They considered the domains for these two approaches that are shown in Fig. 9, right. The shock waves and the mixing layer now have finite thicknesses.

Without going into a lot of detail, I only show the results in Fig. 10, which represents a very impressive picture summarizing a number of very large computations, see [21] [19]. Figure 10 shows a portion of the shock polar diagram of a weak reflection at $M_\infty = 1.73$, $\gamma = 5/3$, $\theta = 13.5°$. The reflected shock polar does not intersect the incident shock polar. The Guderley inviscid solution is indicated by the connection of the two with an expansion wave labelled EW. Results of viscous computations ranging from Reynolds number based on wedge length and free–stream conditions of 2000 to 1.6×10^9 are shown in the form of points representing conditions along the downstream side of the reflected shock and Mach stem. These results show how the connection between the two polars changes smoothly as the Reynolds number is increased, and asymptotically merges into the Guderley solutions as Reynolds number approaches infinity.

The work of the ITAM team under Ivanov that is described in this section represents a brilliant resolution of what has been called the von Neumann Paradox. It explains what happens at finite Reynolds number and shows that the Reynolds number has to be extremely high for the Guderley solution to apply.

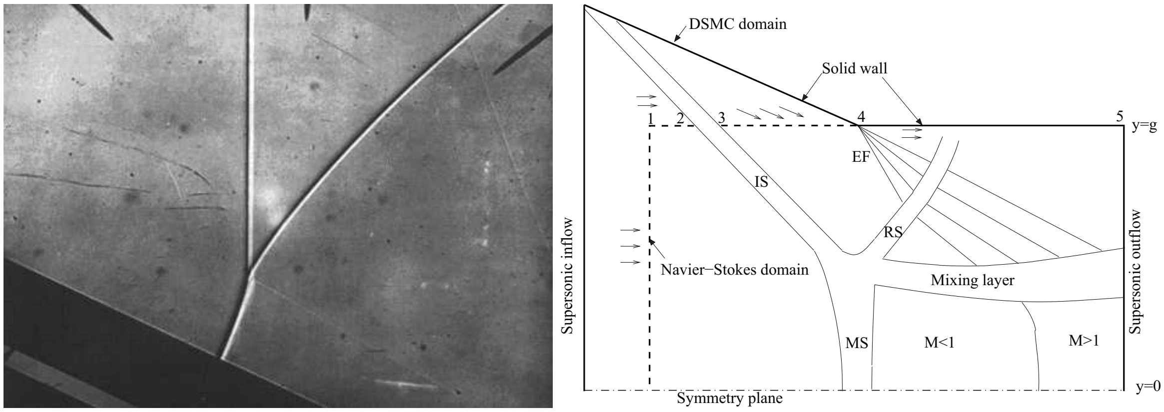

FIGURE 9. Left: L. G. Smith's shadowgraph of weak shock reflection. Reproduced with permission from Physics of Fluids (Sternberg [18]) American Institute of Physics. Right: The domains chosen by Ivanov's team for the viscous computation of the triple point structure using DSMC and Navier–Stokes schemes. Reproduced from Ivanov *et al.* [19] with permission from Elsevier, license no. 3421550792393.

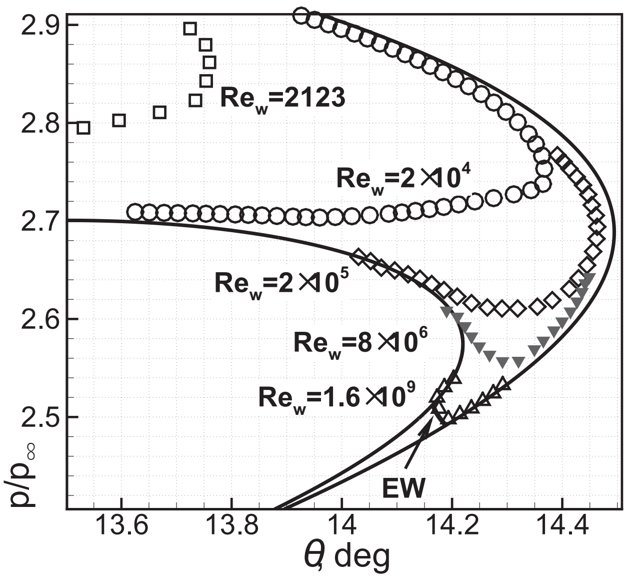

FIGURE 10. Part of the polar diagram for $M_\infty = 1.73$, $\gamma = 5/3$, $\theta = 13.5°$, at which the three–shock theory does not give a solution. The Guderley four wave solution involving an expansion wave centered at the triple point is shown as the line labeled EW. It joins the incident and reflected shock polars. The points show values taken from the downstream side of the Mach stem and reflected shock obtained from numerical solutions at different Reynolds numbers. Note how the manner in which these points join the two polars approaches the Guderley solution as the Reynolds number becomes large. DSMC and Navier–Stokes results show excellent agreement. Reproduced with permission from Shoev G.V., Ivanov M.S., Khotyanovsky D.V., Bondar Y.A., Kudryavtsev A.N.: Supersonic patches in steady irregular reflection of weak shock waves. Editor: K. Kontis, Heidelberg:Springer, 2012, ISBN:978-3-642-25687-5, 28th International Symposium on Shock Waves Vol 2, UK, Manchester, 17 - 22 July 2011, Vol. 1, p. 543-548. License no. 3421560189791.

CALTECH STABILITY EXPERIMENTS

In order to resolve the question of whether, in the dual–solution domain, Mach reflection is more stable than regular reflection, as is implied by the original hysteresis hypothesis and indicated by many of the experimental results, Mouton[17] studied the effect of introducing a disturbance in a regular reflection within the dual–solution domain. However, he first determined the height of the Mach stem theoretically by making some assumptions about

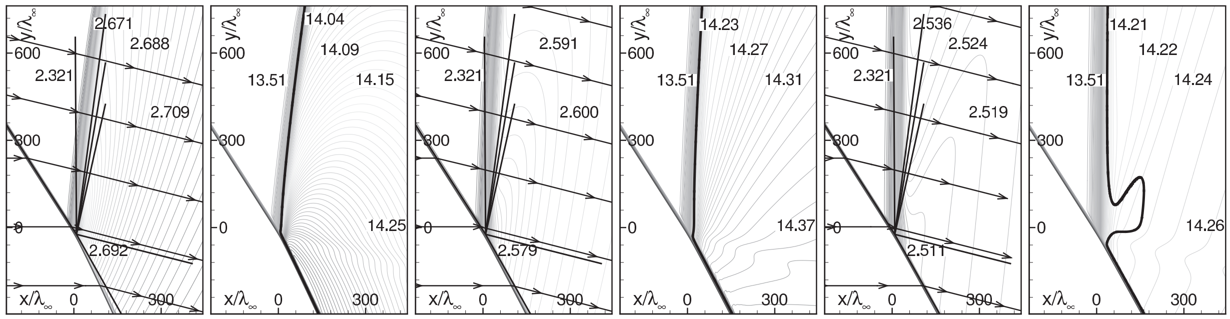

FIGURE 11. These three pairs of figures show lines of constant pressure and lines of constant flow deflection in each pair. Left, middle and right pairs are obtained at Reynolds numbers of 2×10^5, 8×10^6 and 1.6×10^9 respectively. The space coordinates in these figures are normalized by the free–stream mean free path. In this scaling the main effect of the Reynolds number is scaled out. In the left figure of each pair the three shocks and the expansion wave of the Guderley solution are superposed. Note how, as one proceeds to higher Reynolds number, the viscous numerical solution approaches the inviscid Guderley solution. Reproduced with permission from Shoev G.V., Ivanov M.S., Khotyanovsky D.V., Bondar Y.A., Kudryavtsev A.N.: Supersonic patches in steady irregular reflection of weak shock waves. Editor: K. Kontis, Heidelberg:Springer, 2012, ISBN:978-3-642-25687-5, 28th International Symposium on Shock Waves Vol 2, UK, Manchester, 17 - 22 July 2011, Vol. 1, p. 543-548. License no. 3421560189791.

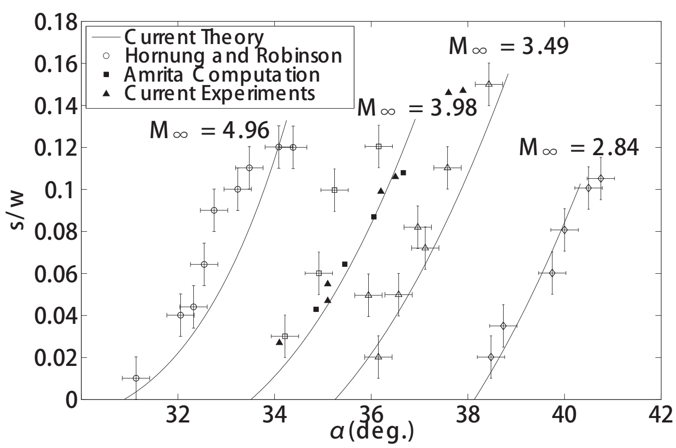

FIGURE 12. Dimensionless Mach stem height plotted vs. shock angle. Results of Hornung and Robinson which failed to show hysteresis. Also shown are the predicted values according to Mouton's[22] theory as well as his experimental and computed results at $M_\infty = 4$.

the structure of a Mach reflection, see [22]. This prediction turned out to be remarkably accurate, as may be seen in Fig. 12.

Mouton prepared his experiments by a numerical study in which a dust particle impinging on one of the wedges in a regular reflection within the dual–solution domain produces a disturbance that is able to trip the reflection to become a Mach reflection. This is shown in the sequence of frames in Fig. 13.

In his experiments, Mouton used an asymmetric arrangement in which one of the wedges was fixed and the other one was able to be rotated. Although the test time in the Ludwieg Tube is only 100 ms, he was able to move the wedge smoothly so that the regular reflection persisted well into the dual–solution domain before jumping to Mach reflection, while, on the reverse path, the Mach reflection changed smoothly into regular reflection, establishing that hysteresis was confirmed.

The next step was to take the reflection into the dual–solution domain and deposit a pulse of energy onto one of the wedge surfaces in order to generate a disturbance that might trip the reflection into a Mach reflection. This was done by focussing a pulsed laser onto one of the wedge surfaces. The result is shown in Fig. 14. Mouton then also analyzed the problem by determining theoretically how much energy would be needed for the trip as a function of the focus location and confirmed the theoretical result computationally.

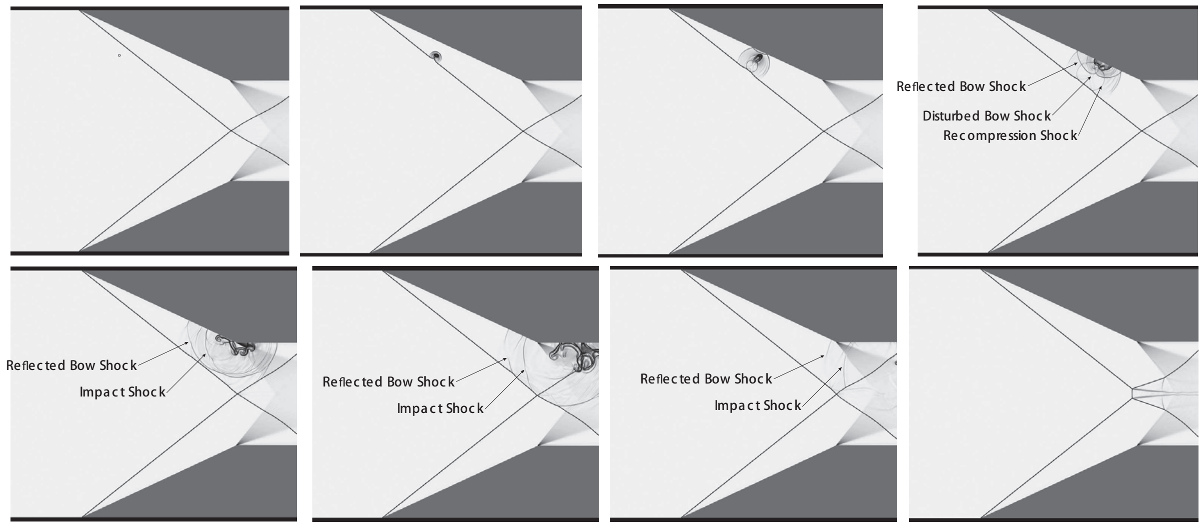

FIGURE 13. Mouton's computations of how the impact of a dust particle on the wedge can produce a shock that can trip a regular reflection in the dual solution domain to flip into a Mach reflection.

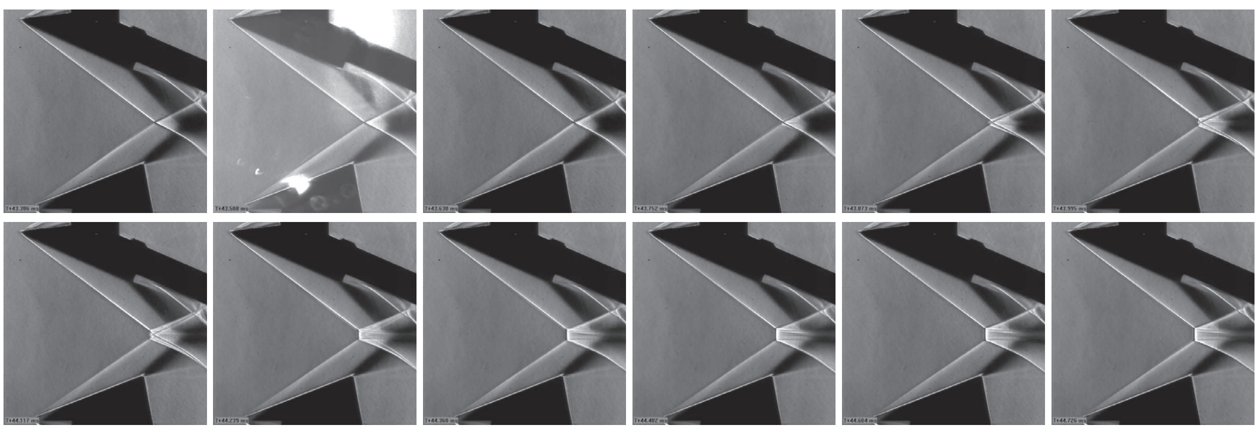

FIGURE 14. Successive frames from a movie taken of flow over two wedges in the Caltech Ludwieg Tube at $M_\infty = 4$. With an initial regular reflection, the condition is taken into the dual solution domain by increasing the angle of one of the wedges. The top left frame shows this condition. Then, in the next frame, a pulsed laser deposits energy on the surface of the bottom wedge. The shock generated by this pulse causes the reflection condition to change to Mach reflection. The time change between the frames is 122 μs.

Finally Mouton was able to determine the growth rate of the Mach stem after such a tripping disturbance both numerically and theoretically, see Fig. 15, left. Fig. 15, right, shows the experimental growth rate in comparison.

One of Mouton's very remarkable results was that, in his Ph. D. thesis, he obtained analytical expressions for the detachment condition, the von Neumann condition and the sonic condition as functions of M_∞ and γ.

All the experimental as well as the computational results have demonstrated that the original hypothesis about hysteresis in Mach reflection, which implies that Mach reflection is more stable than regular reflection in the dual-solution domain is correct. Mouton's experiments confirm it conclusively. Some authors claim that, because regular reflection can exist in the dual–solution domain, it is therefore stable. This argument confuses stability with existence.

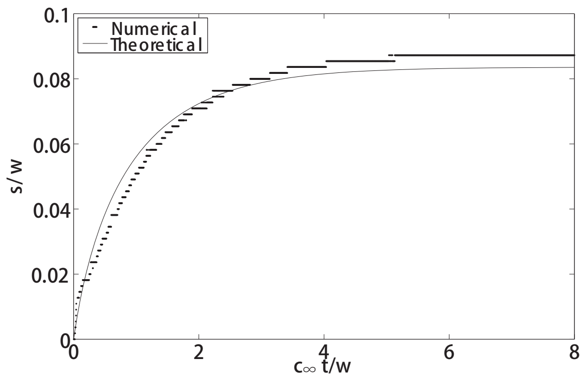

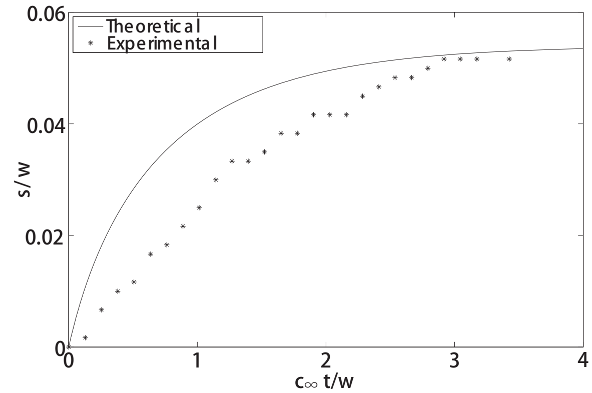

FIGURE 15. Left: Growth rate of the Mach stem after tripping according to computation and Mouton's[22] theoretical prediction. Right: Experimental growth rate. In the experiment the value of w/c_∞ is 240 μs.

CONCLUSIONS

In this paper I have attempted to review the contributions of Mikhail Ivanov and his ITAM team to the problem of steady–flow Mach reflection. Their work on the inviscid regime is exhaustive. Computational and experimental results completely wrap up the problems of hysteresis, three–dimensionality and other effects. Even more remarkable is their resolution of the von Neumann Paradox by explaining the effects of viscosity and heat conduction in a most convincing manner. I end with a presentation of the stability experiments of Mouton, which conclusively show that Mach reflection is more stable than regular reflection in the dual–solution domain.

Mikhail Ivanov was a deeply–thinking scientist whose body of contributions to our field is large and important. But he was also a very good friend with a lively sense of humor and a readiness to enjoy life. It is very sad that we can no longer enjoy his company.

ACKNOWLEDGMENTS

For providing the files for the figures from the publications of Ivanov and his co–workers I wish to thank the Institute of Theoretical and Applied Mechanics of the Siberian Branch of the Russian Academy of Science (ITAM). In particular Y. A. Bondar and G. V. Shoev have helped me enormously. I also wish to acknowledge the technical support of Bahram Valiferdowsi with the experiments in the Caltech Ludwieg Tube. Financial support for the experiments at Caltech was provide by the AFOSR. The AOARD supported my attendance at the Symposium.

REFERENCES

1. H. G. Hornung, H. Oertel, and R. J. Sandeman, *Journal of Fluid Mechanics* **90**, 541–560 (1979).
2. H. G. Hornung, and M. L. Robinson, *Journal of Fluid Mechanics* **123**, 155–164 (1982).
3. M. S. Ivanov, S. F. Gimelshein, and A. E. Beylich, *Physics of Fluids* **7**, 685–687 (1995).
4. M. S. Ivanov, D. Vandromme, V. M. Fomin, A. N. Kudryavtsev, A. Hadjadj, and D. V. Khotyanovskii, *Shock Waves* **11**, 199–207 (2001).
5. M. S. Ivanov, G. P. Klemenkov, A. N. Kudryavtsev, V. M. Fomin, and A. M. Kharitonov, *Doklady Akademii Nauk* **357**, 623–627 (1997).
6. M. S. Ivanov, A. N. Kudryavtsev, S. B. Nikovorov, D. V. Khotyanovskii, and A. A. Pavlov, *Physics of Fluids* **15**, 1807–1810 (2003).
7. M. S. Ivanov, S. F. Gimelshein, and G. N. Markelov, *Computers and Mathemtics with Applications* **35**, 113–125 (1998).
8. M. S. Ivanov, S. F. Gimelshein, and A. N. Kudryavtsev, *Computational Fluid Dynamics '98* **1**, 869–874 (1998).
9. A. N. Kudryavtsev, D. V. Khotyanovskii, M. S. Ivanov, A. Hadjadj, and D. Vandromme, *Shock Waves* **12**, 157–165 (2002).

10. A. V. Trotsyuk, A. N. Kudryavtsev, and M. S. Ivanov, “Mach reflection of shock and detonation waves in steady supersonic chemically reacting flows,” in *Recent Advances in Space Technologies*, edited by F. Ince, and S. Onbasioglu, Turkish Air Force Academy, Istanbul, 2003, pp. 495–503.
11. M. S. Ivanov, G. Ben-Dor, T. Elperin, A. N. Kudryavtsev, and D. V. Khotyanovskii, *AIAA Journal* **39**, 972–974 (2001).
12. A. Hadjaj, A. N. Kudryavtsev, and M. S. Ivanov, *AIAA Journal* **42**, 570–577 (2004).
13. M. S. Ivanov, G. N. Markelov, A. N. Kudryavtsev, and S. F. Gimelshein, *AIAA Journal* **36**, 2079–2086 (1998).
14. M. S. Ivanov, A. N. Kudryavtsev, and D. V. Khotyanovskii, *Doklady Phys.* **45**, 353–357 (2000).
15. M. S. Ivanov, G. Ben-Dor, T. Elperin, A. N. Kudryavtsev, and D. V. Khotyanovskii, *Journal of Fluid Mechanics* **469**, 71–87 (2002).
16. N. Sudani, M. Sato, T. Karasawa, J. Noda, A. Tate, and M. Watanabe, *Journal of Fluid Mechanics* **459**, 167–185 (2002).
17. C. A. Mouton, and H. G. Hornung, *Physics of Fluids* **20** (2008).
18. J. Sternberg, *Physics of Fluids* **2**, 179–206 (1959).
19. M. S. Ivanov, Y. A. Bondar, D. V. Khotyanovskii, A. N. Kudryavtsev, S. B. Nikovorov, and G. V. Shoev, *Progress in Aerospace Sciences* **46**, 89–105 (2010).
20. L. G. Smith, *Physical Review* **69**, 678–678 (1946).
21. D. V. Khotyanovsky, Y. A. Bondar, A. N. Kudryavtsev, G. V. Shoev, and M. S. Ivanov, *AIAA Journal* **47**, 1263–1269 (2009).
22. C. A. Mouton, and H. G. Hornung, *AIAA Journal* **45**, 1977–1987 (2007).